SISSA

PAPER

Direct x-ray detection using thin-film pentacene Schottky diodes

View the article online for updates and enhancements.

Direct x-ray detection using thin-film pentacene Schottky diodes

V. Lakshmi Vineela,[a] **P.A. Praveen,**[b] **T. Kanagasekaran,**[b] **Nitish Kumar C**[a]
and N.V.L. Narasimha Murty[a,*]

[a]*Department of Electrical Engineering, Indian Institute of Technology Tirupati,*
Tirupati 517506, India

[b]*Organic Optoelectronics Research Laboratory, Department of Physics,*
Indian Institute of Sciences Education and Research (IISER) Tirupati,
Tirupati 517507, India

E-mail: nnmurty@iittp.ac.in

Abstract: Direct x-ray detectors using thermally evaporated pentacene thin-films are fabricated in Schottky and coplanar configurations and are analysed for low x-ray dose rates. In both configurations, the x-ray induced photocurrent is found to be five orders of magnitude greater than the theoretically evaluated threshold value that may reflect possible internal gain mechanism. Coplanar detectors showed unstable x-ray photocurrent characteristics; on the other hand, Schottky photodiode structure showed stable response and thus allowed to proceed for x-ray sensitivity measurements. Pentacene-based Schottky detector presented a decent volume sensitivity of $162.3\,\mu C/mGy/cm^3$. The high x-ray sensitivity of pentacene Schottky detector can be due to the complete depletion of the thin-film at the operating reverse bias, revealed by transfer characteristics of fabricated pentacene MESFET. Such a reasonably good x-ray photoconversion in low-Z organic semiconducting materials uncovers the possibility of implementing them in x-ray medical dosimetry applications and in wearable electronic technology.

---

[*]Corresponding author.

Contents

1 Introduction

Radiation is invisible and hence undetectable without a proper device. Utilization of radiation detectors is well-known in the fields of space technology, nuclear power plants, airlines and global security [1, 2]. In addition, radiation detectors find a crucial place in medical imaging, high energy physics, industrial radiography and maintaining global nuclear security by helping in identifying illegal doings over nuclear weapons. It is noteworthy to address x-ray imaging application in detail as imaging based on x-rays is extensively used in clinical radiology. Medical imaging or digital radiography uses large flat-panel system to record patient's x-ray image and displays which are activated by thin-film transistor matrix array [3]. The need for such large area read-out facility is due to the fact that, the digital flat panel imaging must be able to capture complete radiographic image of patient's organ. For instance, in chest radiology the recommended specification of detector size is 43 cm × 43 cm [4]. Conventional semiconductor crystal technology is of little help to cover such extensive area due to limitations imposed by the availability of wafer dimensions and cost constraints [5].

    X-ray detectors operate in two modes: direct and indirect detection. Indirect conversion approach has intermediate scintillation layer that prompts visible photons upon x-ray absorption and the photons are converted to electrical signal by a photodiode. In the case of direct x-ray detection, photoconductor layer directly converts incident x-rays into excess charge. Out of the two configurations, direct conversion possibly has superior resolution and its x-ray imaging panel structure is cost effective to manufacture. The lateral spreading of optical photons in scintillation layer leads to the loss of information and hence is the reason for resolution degradation in indirect approach [6]. General material requirements that should be met for good direct radiation detection are summarized below:

  (i) In case of medical x-ray imaging applications, the photoconductor material should essentially absorb most of the incident energy to mitigate unnecessary radiation exposure on patient. To promote maximum absorption, linear attenuation coefficient (μ_l) must be large in desired energy range or in another way absorption depth δ (reciprocal of μ_l) must be well below the photoconductor thickness.

(ii) The inherent x-ray sensitivity of the material should be eminent, and it depends on single pair creation energy ($E_\pm$). This energy should be low to detect maximum amount of charge (ΔQ) from the absorbed x-ray energy (ΔE).

(iii) Negligible leakage current implies non-injecting contacts, low thermal excitation of carriers from defect states and wide bandgap. The later requirement is in contrary with the condition (ii) which implicitly says low bandgap is required. This trade-off can be balanced if the dark current is $1nA$ at minimum [6].

(iv) The photo generated excess carriers should be collected by the external circuit before they get recombined. For this, charge collection distance, which is the product of mobility, lifetime and electric field ($\mu\tau E$), should be greater than electrode spacing (L) [7].

(v) The material should not degrade with respect to repeated or prolonged exposures of x-rays.

A material which fulfils the above criteria is ideal to work as radiation detector. More frequently used sensor materials in direct detection are based on inorganic semiconductors namely Silicon (Si), high purity Germanium (HPGe), Cadmium Telluride (CdTe), Mercury Iodide (HgI_2), Cadmium Zinc Telluride (CdZnTe) [1, 8] and the only material implemented in commercial x-ray imaging is amorphous Selenium [9]. Though these direct conversion materials assure remarkable detector performance, they have considerable drawbacks as listed below:

(i) They are heavy and mechanically rigid, restricting the ability to design complex flexure structures.

(ii) Developing large area pixelated detector structures for medical imaging is impractical with low-cost requirement as their growth requires exorbitant facilities [10].

(iii) These material's effective atomic number (Z_{eff}) is not consistent with Z_{eff} of biological tissue which is 7.42. This matching is requisite for dosimetry application to evaluate the absorbed dose in biological species under radiation exposure.

Since the aforementioned class of inorganic semiconductors have relatively high atomic number, they are over responsive and hence need a correction factor to obtain absolute value of absorbed dose [11]. Though Diamond ($Z = 6$) is a promising candidate with its near tissue equivalence atomic number, it still holds the complexities in fabrication, constraints on commercially available sizes and cost limitation to implement for large-area applications [12].

These drawbacks can be potentially addressed by a special class of semiconductors called organic semiconductors (OSCs). OSCs are breakthrough materials which reformed the display technology in the recent past with their unique potencies. Enormous research has been carried out in the field of organic electronics targeting at both material and device level. OSC based solar cells, sensors, organic light emitting diodes (OLEDs) and organic field effect transistors (OFETs) are extensively studied in the past decade [13–15]. OLEDs are currently ruling the display technology with the unique feature of flexibility. Though such strenuous work has been carried out in these devices, it is surprising to notice that not much focused activity done on radiation detectors based on organic semiconductors [16]. Exploring this application could unfold interesting observations and novel

possibilities as they have notable advantages. The OSCs offer low fabrication costs and large-area devices, making them attractive materials for medical x-ray imaging. Substrate independent growth allows them to deposit on unconventional substrates like glass, Polyethylene terephthalate (PET), Polyethylene naphthalate (PEN), textiles and kapton tape. This aspect initiates the possibility of fabricating curvy structured detectors that are important in industrial testing [17], radiation leaks in non-planar infrastructures [18], in cone beam computed tomography x-ray imaging and in wearable technology. Solution processed growth allows them to spin coat, dip-coat and even printed using ink-jet printing technology [19, 20]. Basic elemental composition of organic semiconductors being carbon, hydrogen and oxygen makes them human-tissue equivalent. As a result, x-ray detectors made of organic semiconductors can be used to evaluate effective dose received by personnel in radiation prone areas. Moreover, x-ray detectors made out of them can be employed for real-time *in-situ* dose measurements when positioned between x-ray source and patient [21].

Assimilating these advantages, organic semiconductors are not less to be aimed for radiation detection. These benefits motivated the research community to work on radiation detectors and more specifically x-ray dosimeters using organic semiconductor materials as active layer. There are reports on indirect detection using polymer blend P3HT:ICBA and CsI(Tl) as scintillator [22], direct x-ray detection using organic semiconducting crystals [23, 24], polymer based [25–28] and bulk hetero junction polymer based thin films [29–31], small molecule based bi-layer detectors [32, 33]. Effects of x-ray exposure on OFET and their stability were studied with respect to the changes in threshold voltage, surface mobility and radiation hardness [34, 35]. In order to make progress in the x-ray absorption, direct x-ray detection of perovskite based thin-film and crystal devices were studied for medical imaging applications [36–40]. These Perovskite materials lack tissue-equivalence, toxic in nature and hence unsuitable for wearable dosimetry [21]. Recently, Basirico et al., [41] demonstrated direct x-ray detection using solution processed pentacene (TIPS-pentacene) operated at low voltages (less than 1 V) and they observed photoconductive gain in the detection process. Enhanced x-ray absorption by functional group tuning possible for organic semiconductors was addressed by Ciavatti et al. [42]. They synthesized TIPGe by replacing Si atoms in TIPS-pentacene with Germanium whose atomic number is comparatively higher.

Solution-processed thin-film growth involves more process parameters to arrive at uniform films like type of solvent, concentration of solvent to solute and spin cast speed. Though it is reported that TIPS-pentacene has higher mobility than pentacene, because of the massive non-aromatic functional group there exists high anisotropic behavior in TIPS-pentacene. The resistivity of TIPS-pentacene exhibits anisotropy (reported resistivities across a, b and c- axes are 0.5×10^9 Ω·cm, 25×10^5 Ω·cm and, 30×10^9 Ω·cm, respectively) and is lower compared to pentacene whose value is reported as 10^{12} Ω·cm [43]. In general, high resistivity is preferred for a photoconductor material to achieve low leakage current. High surface roughness of TIPS-pentacene is another challenge which is due to thickness deviations during the growth, and this poses difficulty to grow successive layers [44]. In addition, solution processing restricts the choice of opting substrates if they are not chemically stable to particular organic solvent [45]. Most of the device configurations reported on organic thin-films so far are coplanar or gap-type geometries in which both the metal electrodes are on one side of the device with a gap between them called channel length and polymer thick films with operating voltages of few tens to hundreds of volts [25, 26, 28–31, 41]. In coplanar structure, the electric field within the active layer is distributed near to the surface and in general this is beneficial for heavy

radiation particles (such as alpha) detection, as their penetration range in the material is close to the surface compared to x- rays and γ-rays whose penetration depth is deeper [46]. On the other hand, reverse biased Schottky or photodiode structure shows lower dark current as one of the contacts is of blocking type [47]. In the case of Schottky configuration, radiation induced charges are collected by the entire electrode area whereas in coplanar structure, only thin region surrounding electrode boundary participates in charge collection [48].

Pentacene is a p-type benchmark material that has been largely studied in the field of organic electronics with relatively better hole mobilities greater than 1 cm^2/V.s in the thin-film form [49, 50]. Thus, with the combined advantages of thin-film grown pentacene and Schottky configuration, in the present work we have fabricated pentacene based photodiode to detect x-rays directly. As far as we are aware from the literature, this combination is not reported for direct x-ray detection. We could achieve better sensitivity reported so far and this can be attributed to complete depletion of the pentacene Schottky detector.

2 Experimental work

2.1 Film growth and device fabrication

Triple-sublimed grade pentacene ($\geq$ 99.995%) from Sigma-Aldrich [51] was used for the thin-film deposition without any further purification. This high purification grade is one of the purest forms of the pentacene and known to have lesser impurity concentration compared to normal grade material and the resultant devices are expected to have higher mobilities [52]. Interdigitated pre-patterned ITO (work function Φ_m = 4.8 V) coated glass plates with sheet resistance of 20 Ω/sq, variable channel lengths (50 µm, 75 µm, 100 µm, 150 µm, and 200 µm) and 30 mm channel width from Ossila Ltd. were used as substrates. Prior to deposition, the ITO substrates were cleaned by ultra-sonication for 10 min in a lab-based detergent followed by 15 min sonication in acetone, isopropyl alcohol (IPA) and deionized water, respectively. Finally, the substrates were Nitrogen blow dried and kept in a hot air oven at 95°C for 30 min [53]. The substrates were then loaded into a thermal evaporation chamber for the deposition of pentacene films and top contact Aluminum (Al) layer. A 300 nm thick pentacene film was deposited by maintaining the deposition rate around 1 to 1.5 Å/sec and base pressure of 10^{-6} mbar. Using a shadow mask, Al (work function Φ_m = 4.3 V) was deposited on top of pentacene, which forms Schottky contact with pentacene (HOMO edge = 5 eV) [54]. ITO bottom contact pad is of 100 nm thick and top Al contact is of 80 nm thick. The contact structure constitutes an active/sensing area of 4 mm^2. Figure 1 shows the schematic and inset shows the fabricated Schottky device with connection legs for electrical characterization. A single substrate holds five such devices.

Besides the Schottky configuration, bulk photoconductor in coplanar configuration of 0.5 mm^2 active area using pre-patterned ITO interdigitated (IDE) contact pattern is fabricated and the schematic is shown in figure 2. ITO forms ohmic contact with the deposited pentacene thin-film. Out of the channel lengths available on the ITO substrate, we have employed 50 µm channel length device for electrical and x-ray dosimetry studies. The same substrate cleaning procedure as mentioned earlier was followed. In order to compare the photocurrent measurements of both the configurations, we maintained the same thin-film growth parameters like deposition rate, pentacene thickness and
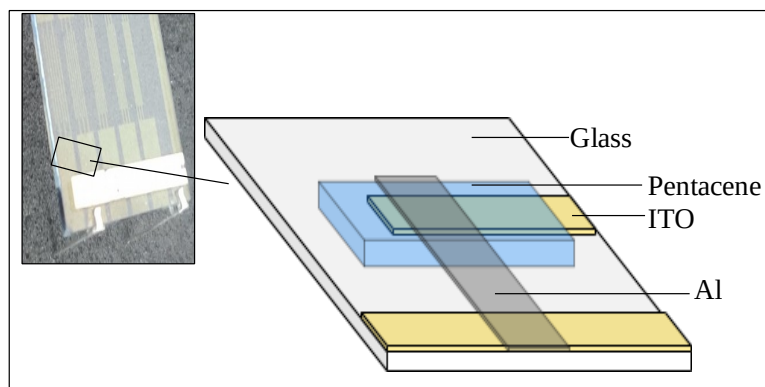
Figure 1. Schematic of the pentacene Schottky device. Inset shows the fabricated device with electrical connection legs at ITO and Al contact pads.

base pressure as that used for the Schottky device. Since IDE electrode structure might lead to higher dark current, it has to be balanced by properly assessing the active geometry of the semiconductor layer. That means, smaller active area might suppress the leakage current at the same time reduces the radiation sensing area. Finally, the devices are connected with electrical connection legs in order to proceed for electrical characterization.
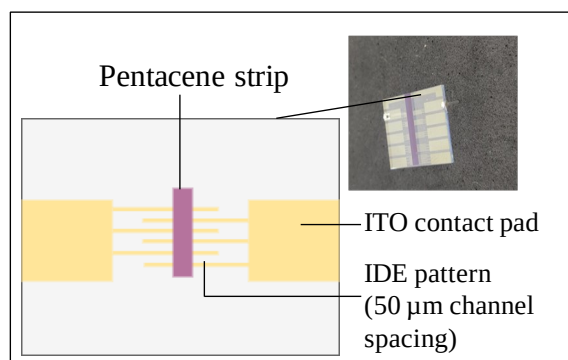
Figure 2. Schematic of the pentacene coplanar device. Inset shows the fabricated device with connection legs at ITO pads.

2.2   Electrical characterization and X-ray dosimetry studies

Steady-state and time dependent electrical measurements were performed at ambient conditions using Keithley 2410 source meter by mounting the detector onto its associated test fixture. For Schottky detector, voltage was applied to the ITO contact pads by grounding Al cathode. X-ray detection studies were done using Leybold x-ray apparatus which has three sections: high voltage and display section, x-ray tube with Molybdenum anode (whose characteristic x-ray peaks occur at $17.4\,\text{keV}$ K_α, $19.6\,\text{keV}$ K_β) and the experimentation chamber. The x-ray tube voltage can be varied between 0 to $35\,\text{kV}$ and tube current between 0 to $1\,\text{mA}$. The calculated dose rate values vary between 0.1 to $0.877\,\text{mGy/sec}$ at a distance of $2.5\,\text{cm}$ between the detector and collimator. Dosimetry measurements were conducted by mounting the detector on a test fixture that is $2.5\,\text{cm}$

away from the x-ray beam slit, inside the experimentation chamber. The fabricated detectors are placed such that the x-rays incident on the device from the Al contact side for Schottky and are directly incident on to the pentacene for coplanar configuration. The chamber is equipped with automatic door interlock system when x-ray source is ON, for safety purpose.

3 Results and discussion

Ionization capability of x-rays upon impinging on solid-state detectors through scattering or by photoelectric absorption is utilized for direct x-ray detection. The deposited x-ray photon creates many free charges upon traversing the active volume of detector. Charge collection of photo generated carries by applied electric field constitute x-ray induced photocurrent in the detector. To assess the upper limit on x-ray photocurrent generation capability of pentacene, theoretical quantum efficiency calculations are carried out using its mass attenuation coefficient (μ_m) [55]. Considering the exponential decay of photon beam while traversing the active layer thickness, initial intensity of the x-ray beam I_0, depth of absorber material (d) and linear attenuation coefficient μ_l are related to transmitted intensity I as:

$$I = I_o e^{-\mu_l d} \tag{3.1}$$

In medical physics, the percentage of incident photons attenuated (not necessarily absorbed) within the photoconductor material can be evaluated theoretically using quantum efficiency (QE), if the material's density (ρ) and mass attenuation coefficient (μ_m) at that particular incident energy are known and is given as:

$$QE = (1 - e^{-\mu_m \rho d}) \tag{3.2}$$

Mass attenuation coefficient of pentacene at different energies is simulated using XCOM code [56] and quantum efficiencies (in %) at 10 keV, 17.599 keV, 20 keV, 50 keV, 100 keV and 500 keV is evaluated in the thickness range 1 nm to 10 μm and is shown in figure 3. The plot clearly depicts that the quantum efficiency increases with the thickness of photoconductor material. But increasing thickness alone to achieve better absorption is not a substantial way, particularly for single layer
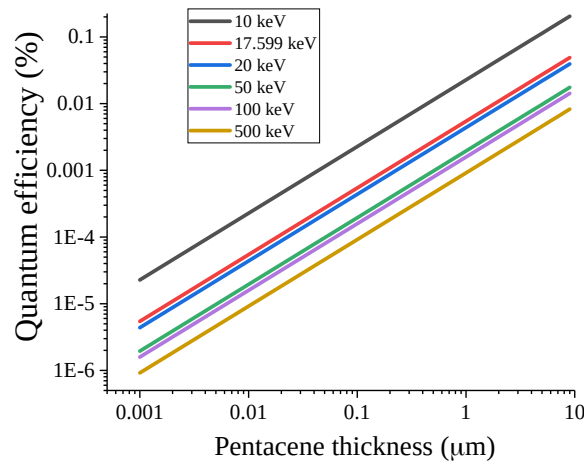
Figure 3. Plot of theoretical quantum efficiency as function of pentacene thickness at different x-ray energies.

organic semiconductors as they pose challenges like low exciton diffusion length, high electric field, morphological issues while growing thicker layers and low carrier mobility [57]. This ideal quantum efficiency gives an estimate on maximum possible theoretical photocurrent that can be achieved upon x-ray exposure, under the assumption that all the photons attenuated are absorbed. This theoretically obtained value sets out as a reference to analyze the experimentally observed photoresponse.

Figure 4 shows the plot of measured dark and x-ray photo current response of the pentacene Schottky diode. The dark current in forward bias was much higher than the dark current in reverse bias which reveals that the current conduction was dominant in one direction. The rectification factor [58] which is the ratio of forward to reverse current at particular voltage was found to be 209 at 4 V/−4 V and was gradually diminishing to 98 at 3 V/−3 V, 43 at 2 V/−2 V, 1.15 at 1 V/−1 V. The measured dark current was of the order of 10^{-10} A up to −4 V reverse voltage. Noticeable increase in the x-ray photoresponse was observed in reverse bias whereas in the forward bias both dark and photocurrents were found overlapping. This observation confirms that reverse bias is the appropriate region for x-ray detection for the Schottky configuration and photo-current was recorded even at 0 V which signifies the photo-voltaic mode of detector operation. Secondary electrons that are created due to the interaction of x-ray photons with the top Al metal contact will cause ionization in the first few tens of nanometer thick pentacene. This could implicitly enhance the x-ray induced current known as dose enhancement effect [41]. Figure 5 shows the dark and x-ray response for the coplanar configuration. Though not shown here, we observed space charge limited current characteristics (SCLC) [59] in case of coplanar configuration, when the device was swept for higher voltages up to 150 V and the hole mobility extracted from the trap-free region was found to be 3.31 cm^2/V·s. The dark current for the coplanar detector was an order higher compared to the Schottky detector in reverse bias. The photo-response for the coplanar configuration was insignificant at low voltages and a progressive increase was noticed with applied bias. It was noticed (figure 5) that the background contribution of photocurrent to the impinging x-rays without pentacene thin-film was an order of magnitude lesser compared to the photocurrent with the active layer. Hence, the x-ray photocurrent contribution of the substrate and the contacts is negligible.
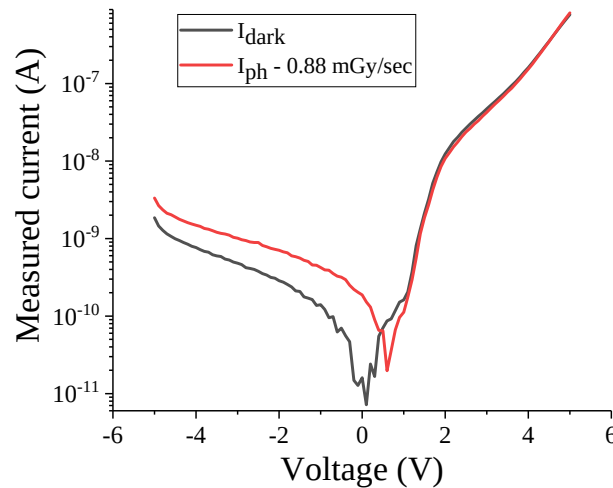
Figure 4. Dark current (I_{dark}) and photo current (I_{ph}) of Schottky diode at a dose rate of 0.8778 mGy/sec for 60 sec of x-ray exposure.
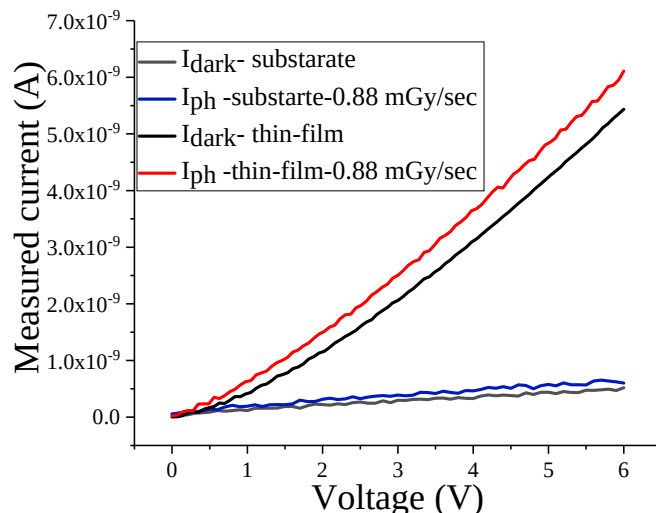
Figure 5. Dark current (I_{dark}) and photo current (I_{ph}) of coplanar device (50μm channel length) with and without pentacene layer at a dose rate of 0.8778 mGy/sec for 60 sec x-ray exposure.

Though pentacene showed measurable sensitivity in both configurations, the minimum leakage current criteria was met by the Schottky detector in comparison with the coplanar configuration. To examine the stability of dark currents in both configurations, we measured dark (I_{dark}) and x-ray photocurrent (I_{ph}) response under various dose rates which are shown in figures 6 and 7. X-ray photocurrents were found to increase with dose rates in both the detector configurations whereas coplanar configuration showed deterioration in dark currents (figure 6) that were measured at each instant of x-ray dose exposure. The coefficient of variation (CV) for the coplanar detectors is observed to be greater than 50%. Similar unstable response was observed for the other channel lengths as well. The possible reason for the degradation in dark currents could be the direct exposure of pentacene thin film to ambient conditions that might lead to photo-oxidation, ultimately creating surface defects [24].
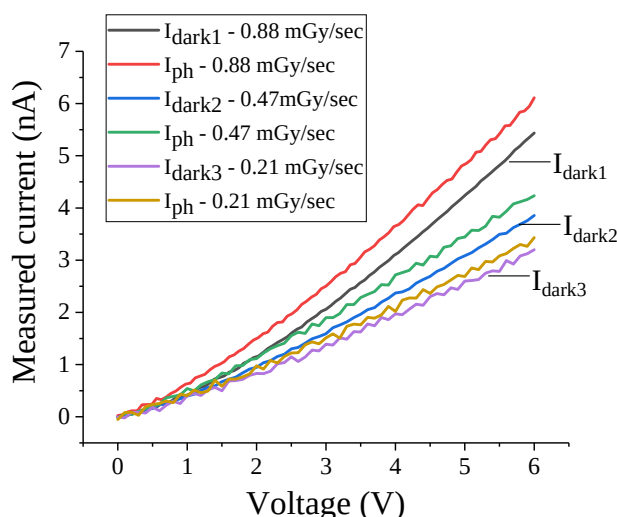
Figure 6. Dark (I_{dark}) and photocurrents (I_{ph}) of pentacene coplanar device for varying x-ray dose.
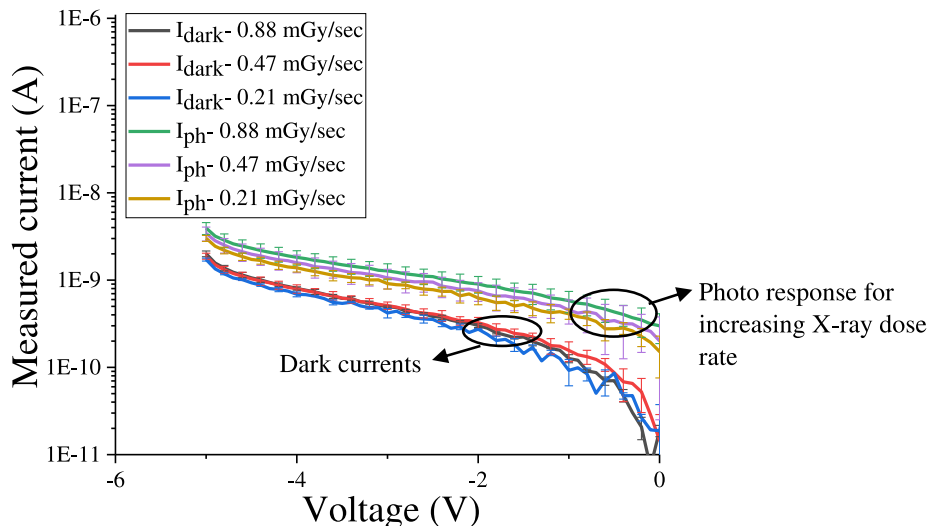
Figure 7. Dark (I_{dark}) and photo currents (I_{ph}) of the pentacene Schottky diode for varying x-ray dose.

This did not happen in case of the Schottky detector as it has the top electrode which to some extent may act as an encapsulant to the underlying pentacene layer. Oxidation of pentacene leads to the disruption of its π conjugation system because of which transfer of charge carriers between the molecules get inhibited [60]. In the Schottky configuration, dark current was found to be stable (figure 7) and it is a favorable feature for detector as it in turn does not introduces uncertainty in the measured photocurrent. In case of the Schottky detector, internal electric field across the depletion region assists the charge carrier separation in addition to the external applied bias. To confirm the extent of depletion region in the pentacene Schottky diode, we fabricated Metal-Semiconductor Field Effect Transistor (MESFET) structure by thermally evaporating Al metal on top of the pentacene layer in coplanar configuration and it acts as a gate contact. The fabricated structure is a bottom contact- top gate type, with a channel length (L) of 50 μm and width (W) of 10 mm. Figure 8 shows the plot of transfer characteristics of the fabricated pentacene MESFET. The $I_{\text{ds}} - V_{\text{gs}}$ characteristics reveal a threshold voltage of -5 V which confirms that the entire pentacene thickness (300 nm) is depleted even at 0 V and the device operates in normally-off mode. Since the device is an enhancement mode MESFET, forward biasing (< -5 V) of gate- source Schottky junction is needed for appreciable current. It is evident from figure 8 that for the entire reverse bias operation of the Schottky detector, the depletion region completely covers the electrode spacing. This may be reason for better photo-response in case of the Schottky configuration compared to coplanar configuration.

The measured x-ray induced photocurrent in both the configurations was found to be five orders of magnitude greater than the theoretical upper limit. The maximum theoretical photocurrent can be calculated by considering mass-attenuation coefficient of pentacene at 17.5 keV which is 0.54478 cm^2/g, density of pentacene as 1.32 g/cm^3, attenuation depth of the incoming x-ray beam in 300 nm thick pentacene and incident photon flux (Ψ_0) and by using the conversion formula between the absorbed dose for a photon source and photon flux, it is likely to find out the incident photon flux [62],

$$\Psi_o = \frac{DA}{E_{\text{ph}}\mu_{\text{m-air}}} \tag{3.3}$$
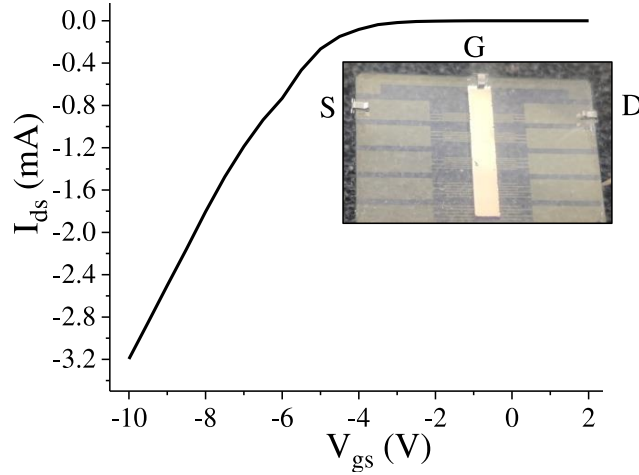
Figure 8. Drain current (I_{ds}) vs gate voltage (V_{gs}) of the pentacene MESFET and the inset shows fabricated device with connection legs at source (S), drain (D) and gate (G).

where D is the dose rate, A is the active area of the detector, E_{ph} is the incoming x-ray energy and $\mu_{m\text{-air}}$ is the mass-attenuation coefficient of air.

Considering the maximum dose rate of 0.88 mGy/sec, the active area of the Schottky detector as 4 mm^2, energy of x-ray radiation as 17.5 keV, mass-attenuation coefficient of air as 1.14 cm^2/g and converting *Gray* to Joule/Kg, we obtain Ψ_0 as 1.1×10^7 photons/sec. The percentage of photon attenuation in 300 nm thick pentacene is found to be 0.0022%. Assuming this total fraction of photons attenuated are absorbed within the active layer thickness, the theoretical maximum photocurrent value was estimated to be less than 10^{-15} A. Similar range of values were observed by Basirico et al. [41] for TIPS-Pentacene based direct x-ray detectors. The experimentally observed magnitude of the x-ray photocurrent was in nanoamperes and it clearly crossed the utmost theoretically computed photocurrent value by significant margin in our case as well.

This can be accredited to the photoconductive gain mechanism taking place in the pentacene thin film during the process of electron-hole pair generation and collection. When excess charge carrier pairs are created by x-ray radiation, conductivity of the thin film accentuates and the photocurrent starts to flow with the application of electric bias [63]. The photoconductive response (I_{ph}) is given by,

$$I_{ph} = q\Psi_o\eta G \tag{3.4}$$

where Ψ_0 is the number of incident photons per unit time, η is the quantum efficiency that lies between 0 and 1 and G is photoconductive gain given by the ratio of charge collection distance ($L_c = \mu\tau E$) and the electrode separation (L) [64]. Therefore, from eq. (3.4) the amount of photocurrent will increase with increase in the applied electric field, by reducing channel spacing and it also depends on carrier lifetime. Loss of charges due to recombination or trapping, results in reduction of measurable current at the electrodes. The observation in our case clearly project; gain factor (G) must probably be greater than unity that led measured photocurrent to be five orders of magnitude greater than the theoretical upper limit. G greater than 1 indicates, photo induced holes drifting across the thin film several times without being recombined with electrons [65]. Here we say holes because pentacene is a p-type material and hence holes are the dominant charge carriers with mobility higher than electrons. On the

other hand, trapping of electrons also lead to increase in photoconductive gain. When an electron gets trapped at defect site, external circuit has to supply additional opposite type of carriers with the aim of preserving charge neutrality. This leads to alternative means of hole generation in the pentacene thin-film besides photo generated holes and hence adds to photoconductive gain mechanism.

Figures 9 and 10 shows the detector response to ON-OFF x-ray exposure cycles at the dose rate of 0.47 mGy/sec for the Schottky and the coplanar detector configurations at −4 V and 5 V applied bias, respectively. The Schottky detector performance was checked even at 0 V and no stable response was observed, which means the electric field might not be sufficient for complete charge collection. Drift in the dark current was noticed for the coplanar device (figure 10) and it is justified by the similar instability found while taking current-voltage measurements as well (figure 7). Also the uncertainties in the measured data for coplanar devices are found to be higher (CV >> 40%) compared to Schottky devices. Similar trend was reported in rubrene and perovskite single crystal materials for planar configuration [24, 66]. But the Schottky detector did not exhibit such instability as seen in figure 9.
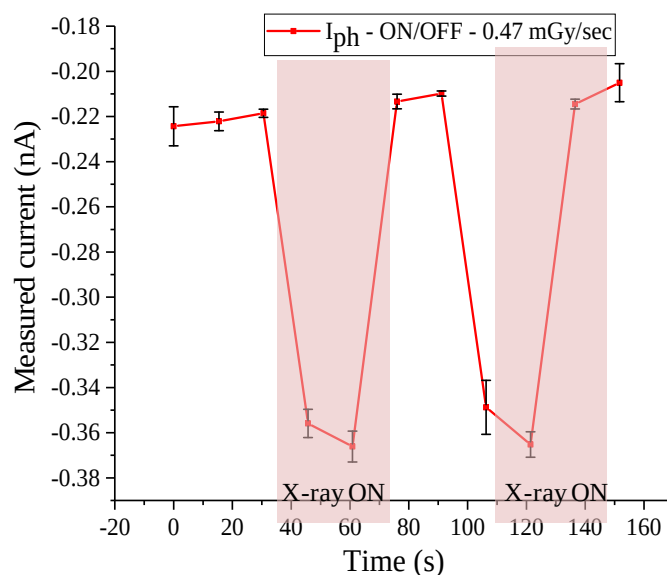
Figure 9. Dynamic response of the pentacene schottky detector at the x-ray dose rate of 0.47 mGy/sec at −4 V.

The Schottky configuration (contacts are in top-bottom fashion) is more capable of collecting photo generated charges due to its uniform electric field effectively covering the whole electrode region. Also the built-in potential in the Schottky device aids in the drift of photo generated charge carriers towards their respective electrodes without getting greatly recombined compared to the coplanar configuration. In coplanar configuration, electric field gets modified throughout the channel because of the highest possibility of space charge effect that certainly happens in case of injection contacts [67]. Also, in addition to the defects originating due to x-ray exposure in both configurations, coplanar configuration has direct impact of environment on thin-film making it more sensitive to oxidation. These could be the probable and possible reasons for unstable performance of the coplanar detector configuration. In general, stability in dark current is one of the major factors that serve to the detector's linearity and the devices with space charge effects will probably fail to show the linear behavior [68]. Thus the coplanar configuration is not further studied for x-ray sensitivity analysis.
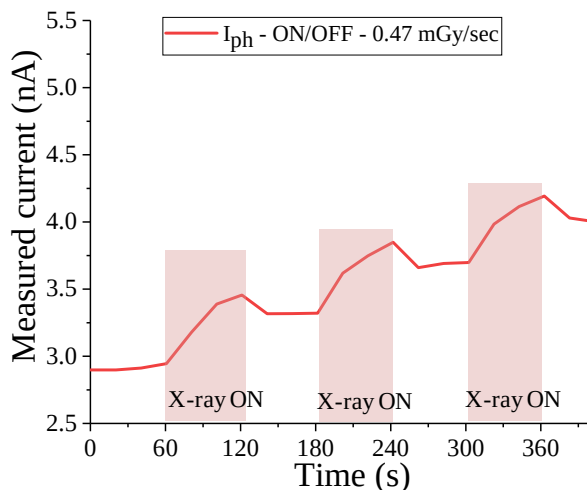
Figure 10. Dynamic response of the pentacene coplanar detector at the x-ray dose rate of 0.47 mGy/sec at 5 V.

By adjusting the x-ray tube current, photo response ($I_{ph} - I_{dark}$) at different x-ray dose rates was examined for pentacene Schottky detector at -4 V applied bias for different x-ray exposure times and is shown in figure 11. It was observed that photocurrent increased with increase in dose rate nearly in a linear fashion. The detector was then exposed for different time intervals of 20 sec, 30 sec and 60 sec, to see the changes in photocurrent signal. With increase in exposure time, the photocurrent response was found to increase as depicted in figure 11. By linear fitting of the above graph to the photo response values, sensitivity of the detector can be determined which is defined as $S = (I_{ph} - I_{dark})/D$; where D is the x-ray dose rate.
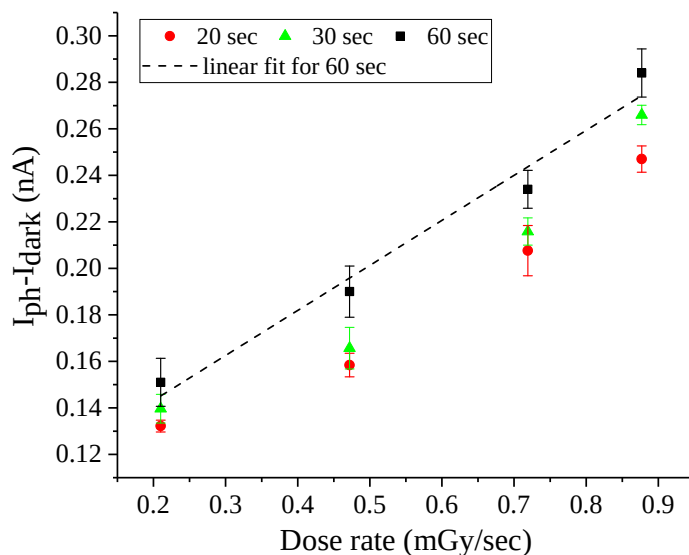
Figure 11. X-ray dose rate dependent photocurrent of the Schottky detector at -4 V bias for different exposure times.

The minimum sensitivity calculated for 60 sec of x-ray dose exposure through linear fit of the experimental data (shown by the dotted line of figure11) was found to be 194.8 nC/Gy (range:

194.8–220 nC/Gy). In terms of sensitivity per unit volume with thickness of pentacene being 300 nm, it is 162.3 µC/mGy/cm^3 (range: 162.3–183.3 µC/mGy/cm^3) and it is an appreciable value compared to the reported sensitivities. The reason for such high volume sensitivity can be attributed to the pentacene layer getting fully depleted at the detector operating voltage of −4 V as seen from the transfer characteristics of MESFET plotted in figure 8. This might have led to the effective collection of photo generated charge carriers within the active layer in Schottky configuration. As a comparison with the sensitivity values reported so far for OSC based direct x-ray detector, table 1 gives the summary. From table 1, the proposed pentacene Schottky detector has shown higher volume sensitivity compared the reported works. However, detector fabrication on flexible substrates, detector encapsulation and optimized performance at zero bias operation needs further investigation.

Table 1. Comparison of organic semiconductor based direct x-ray detectors.

Material(s)	Thickness (µm)	Active area (mm^2)	Voltage (V)	Sensitivity (nC/Gy)	Sensitivity (µC/mGy/cm^3)	Reference
Poly(9,9-dioctylfluorene) (PFO)	20	25	−10	—	0.128	[25]
Poly [1-methoxy-4-(2-ethylhexyloxy)-phenylenevinylene] (MEH-PPV)	20	25	−10		0.2	[25]
Poly (triarylamine) (PTAA)	30	25	−300	—	0.4	[28]
Poly([9,9-dioctyfluorenyl-2,7-diyl]-co-bithiophene) (F8T2)	10	25	−150	—	0.02	[69]
P3HT:PCBM (Indirect detection)	—	4	−0.6	54×10^3	—	[22]
ITO/PTAA/Al	30	25	−300	—	0.132	[27]
ITO/PTAA/Au	30	25	300		0.204	[27]
DNN crystal	—	—	5	3.3	—	[24]
Rubrene crystal	—	—	5	1.4		
TIPS-Pentacene	0.1	1.5	0.2	180	72	[41]
TIPS-Pentacene (OFET)	0.1	—	−3	1200	—	[70]
Pentacene	0.3	4	−4	194.8*	162.3*	This Work

* Indicates the minimum sensitivities determined from figure 11.

4 Conclusions

Direct x-ray detection based on thermally evaporated pentacene in both Schottky and coplanar device configurations was explored. It was observed that, the Schottky detector presented stable operating condition as x-ray detector without exhibiting drift in dark current, in comparison with the coplanar configuration. This can be attributed to the structural advantages that Schottky devices have. Schottky structure to a considerable extent maintains conformity between electron-hole pair

generation, their drift and recombination which is crucial for obtaining efficient photocurrent signal. Its internal space charge region has built-in electric field that aids in rapidly dissociating the x-ray induced charge carriers generated within, there by significantly reducing the recombination. Also the top metal provides a sort of encapsulation to the active layer beneath, that helps in minimizing the direct environmental damage to the surface mono-layers. Embedding these intrinsic capabilities of the fabricated Schottky structure, we could achieve appreciable minimum volume sensitivity of 162.3 μC/mGy/cm^3 at even low dose rate of 0.88 mGy/sec. This could be possible because of the photodiode structure leading to complete active layer thickness depletion which is complemented by the measured transfer characteristics of the pentacene MESFET. Hence, thermally evaporated pentacene based Schottky detector can be promising for direct x-ray detection in medical dosimetry.

References

[1] P.M. Johns and J.C. Nino, *Room temperature semiconductor detectors for nuclear security*, *J. Appl. Phys.* **126** (2019) 40902.

[2] H. Liang, S. Cui, R. Su, P. Guan, Y. He, L. Yang et al., *Flexible X-ray detectors based on amorphous Ga2O3 thin films*, *ACS Photonics* **6** (2018) 351.

[3] A.R. Cowen, S.M. Kengyelics and A.G. Davies, *Solid-state, flat-panel, digital radiography detectors and their physical imaging characteristics*, *Clin. Radiol.* **63** (2008) 487.

[4] K. Bacher, P. Smeets, L. Vereecken, A. De Hauwere, P. Duyck, R. De Man et al., *Image quality and radiation dose on digital chest imaging: comparison of amorphous silicon and amorphous selenium flat-panel systems*, *Am. J. Roentgenol.* **187** (2006) 630.

[5] G.F. Knoll, *Radiation Detection and Measurement*, John Wiley & Sons (2010).

[6] S.O. Kasap and J.A. Rowlands, *Direct-conversion flat-panel X-ray image sensors for digital radiography*, *Proc. IEEE* **90** (2002) 591.

[7] C. Wang, X. Du, S. Wang, H. Deng, C. Chen, G. Niu et al., *Sb 2 Se 3 film with grain size over 10 μm toward X-ray detection*, *Front. Optoelectron.* (2020) 1.

[8] G. Ariño-Estrada et al., *Measurement of mobility and lifetime of electrons and holes in a Schottky CdTe diode*, 2014 *JINST* **9** C12032.

[9] B.D. Milbrath, A.J. Peurrung, M. Bliss and W.J. Weber, *Radiation detector materials: An overview*, *J. Mater. Res.* **23** (2008) 2561.

[10] A. Datta, Z. Zhong and S. Motakef, *A new generation of direct X-ray detectors for medical and synchrotron imaging applications*, *Sci. Rep.* **10** (2020) 1.

[11] C. Furetta, M. Prokic, R. Salamon, V. Prokic and G. Kitis, *Dosimetric characteristics of tissue equivalent thermoluminescent solid TL detectors based on lithium borate*, *Nucl. Instrum. Meth. A* **456** (2001) 411.

[12] S.P. Lansley, G. T. Betzel, J. Meyer, F. Baluti and L. Reinisch, *CVD Diamond X-Ray Detectors for Radiotherapy Dosimetry*, in proceedings of *IEEE SENSORS*, Christchurch, New Zealand, 25–28 October 2009, pp. 1238–1243.

[13] B. Canımkurbey et al., *Medium band gap polymer based solution-processed high-κ composite gate dielectrics for ambipolar OFET*, *J. Phys. D* **51** (2018) 125104.

[14] J. Oh et al., *Bending performance of flexible organic thin-film transistors with/without encapsulation layer*, *IEEE Trans. Device Mater. Reliab.* **18** (2017) 1.

[15] Y. Guo, G. Yu and Y. Liu, *Functional organic field-effect transistors*, *Adv. Mater.* **22** (2010) 4427.

[16] J.-S. Park, H. Chae, H.K. Chung and S.I. Lee, *Thin film encapsulation for flexible AM-OLED: a review*, *Semicond. Sci. Technol.* **26** (2011) 34001.

[17] L. Basiricò, A. Ciavatti and B. Fraboni, *Solution-Grown Organic and Perovskite X-Ray Detectors: A New Paradigm for the Direct Detection of Ionizing Radiation*, *Adv. Mater. Technol.* **6** (2021) 2000475.

[18] C.S. Schuster, B.R. Smith, B.J. Sanderson, J.T. Mullins, J. Atkins, P. Joshi et al., *Flexible silicon-based alpha-particle detector*, *Appl. Phys. Lett.* **111** (2017) 73505.

[19] S.E. Root, S. Savagatrup, A.D. Printz, D. Rodriquez and D.J. Lipomi, *Mechanical properties of organic semiconductors for stretchable, highly flexible, and mechanically robust electronics*, *Chem. Rev.* **117** (2017) 6467.

[20] J.A. Posar, J. Davis, M.J. Large, L. Basiricò, A. Ciavatti, B. Fraboni et al., *Characterization of an organic semiconductor diode for dosimetry in radiotherapy*, *Med. Phys.* **47** (2020) 3658.

[21] L. Basiricò, A. Ciavatti, I. Fratelli, D. Dreossi, G. Tromba, S. Lai et al., *Medical applications of tissue-equivalent, organic-based flexible direct X-ray detectors*, *Front. Phys.* **8** (2020) 13.

[22] H. Seon, B. Kim and J. Kang, *Characteristic of an Organic Photodetector fabricated with P3HT: ICBA blending materials for Indirect X-ray Detection*, *IEEE Trans. Nucl. Sci.* **64** (2016) 1739.

[23] B. Fraboni, A. Ciavatti, F. Merlo, L. Pasquini, A. Cavallini, A. Quaranta et al., *Organic Semiconducting Single Crystals as Next Generation of Low-Cost, Room-Temperature Electrical X-ray Detectors*, *Adv. Mater.* **24** (2012) 2289.

[24] L. Basiricò et al., *Solid state organic X-ray detectors based on rubrene single crystals*, *IEEE Trans. Nucl. Sci.* **62** (2015) 1791.

[25] F.A. Boroumand, M. Zhu, A.B. Dalton, J.L. Keddie, P.J. Sellin and J.J. Gutierrez, *Direct x-ray detection with conjugated polymer devices*, *Appl. Phys. Lett.* **91** (2007) 33509.

[26] C.A. Mills, A. Intaniwet, M. Shkunov, J.L. Keddie and P.J. Sellin, *Flexible Radiation Dosimeters Incorporating Semiconducting Polymer Thick Films*, *Proc. SPIE* **7449** (2009) 74491I.

[27] A. Intaniwet, C.A. Mills, P.J. Sellin, M. Shkunov and J.L. Keddie, *Achieving a stable time response in polymeric radiation sensors under charge injection by X-rays*, *ACS Appl. Mater. Interfaces* **2** (2010) 1692.

[28] A. Intaniwet, C.A. Mills, M. Shkunov, H. Thiem, J.L. Keddie and P.J. Sellin, *Characterization of thick film poly (triarylamine) semiconductor diodes for direct x-ray detection*, *J. Appl. Phys.* **106** (2009) 64513.

[29] T. Agostinelli. M. Campoy-Quiles. J.C. Blakesley. R. Speller. D.D.C. Bradle. an. J. Nelson, *A polymer/fullerene based photodetector with extremely low dark current for x-ray medical imaging applications*, *Appl. Phys. Lett.* **93** (2008) 419.

[30] P.E. Keivanidis, N.C. Greenham, H. Sirringhaus, R.H. Friend, J.C. Blakesley, R. Speller et al., *X-ray stability and response of polymeric photodiodes for imaging applications*, *Appl. Phys. Lett.* **92** (2008) 13.

[31] A. Intaniwet, J.L. Keddie, M. Shkunov and P.J. Sellin, *High charge-carrier mobilities in blends of poly (triarylamine) and TIPS-pentacene leading to better performing X-ray sensors*, *Org. Electron.* **12** (2011) 1903.

[32] M. Koželj and B. Cvikl, *On the Possibilities of Neutron Detection with Organic Semiconductor Structures*, in proceedings of the in *21st International Conference Nuclear Energy for New Europe*, Ljubljana, Slovenia, 5–7 September 2012 [https://arhiv.djs.si/proc/nene2012/Publication_datoteke/Proceedings/1010.pdf].

[33] E. Takada, A. Inoue, H. Imai, H. Okada, S. Naka and J. Kawarabayashi, *Application of a Heterojunction Organic Photodiode to Radiation Measurement*, *IEEE Nucl. Sci. Symp. Conf. Rec.* **2009** (2009) 1295.

[34] R.A.B. Devine, M.-M. Ling, A.B. Mallik, M. Roberts and Z. Bao, *X-ray irradiation effects in top contact, pentacene based field effect transistors for space related applications*, *Appl. Phys. Lett.* **88** (2006) 151907.

[35] C.R. Newman, H. Sirringhaus, J.C. Blakesley and R. Speller, *Stability of polymeric thin film transistors for x-ray imaging applications*, *Appl. Phys. Lett.* **91** (2007) 142105.

[36] H.S. Gill, B. Elshahat, A. Kokil, L. Li, R. Mosurkal, P. Zygmanski et al., *Flexible perovskite based X-ray detectors for dose monitoring in medical imaging applications*, *Phys. Med.* **5** (2018) 20.

[37] H. Wei, Y. Fang, P. Mulligan, W. Chuirazzi, H.-H. Fang, C. Wang et al., *Sensitive X-ray detectors made of methylammonium lead tribromide perovskite single crystals*, *Nat. Photonics* **10** (2016) 333.

[38] X. Geng, Q. Feng, R. Zhao, T. Hirtz, G. Dun, Z. Yan et al., *High-quality single crystal perovskite for highly sensitive X-ray detector*, *IEEE Electron Device Lett.* **41** (2019) 256.

[39] Y.C. Kim, K.H. Kim, D.-Y. Son, D.-N. Jeong, J.-Y. Seo et al., *Printable organometallic perovskite enables large-area, low-dose X-ray imaging*, *Nature* **550** (2017) 87.

[40] B. Náfrádi, G. Náfrádi, L. Forró and E. Horváth, *Methylammonium lead iodide for efficient X-ray energy conversion*, *J. Phys. Chem. C* **119** (2015) 25204.

[41] L. Basirico, A. Ciavatti, T. Cramer, P. Cosseddu, A. Bonfiglio and B. Fraboni, *Direct X-ray photoconversion in flexible organic thin film devices operated below 1 V*, *Nat. Commun.* **7** (2016) 1.

[42] A. Ciavatti, L. Basiricò, I. Fratelli, S. Lai, P. Cosseddu, A. Bonfiglio et al., *Boosting direct X-ray detection in organic thin films by small molecules tailoring*, *Adv. Funct. Mater.* **29** (2019) 1806119.

[43] J. Chen, D.C. Martin and J.E. Anthony, *Morphology and molecular orientation of thin-film bis (triisopropylsilylethynyl) pentacene*, *J. Mater. Res.* **22** (2007) 1701.

[44] K. Asare-Yeboah, *Temperature gradient approach to grow preferentially-oriented tips pentacene crystals for organic thin film transistors*, Doctoral dissertation, The University of Alabama (2015) [https://ir.ua.edu/handle/123456789/2508].

[45] F. Cicoira and C. Santato, *Organic Electronics: Emerging Concepts and Technologies*, John Wiley & Sons (2013).

[46] A. Mainwood, *Recent developments of diamond detectors for particles and UV radiation*, *Semicond. Sci. Technol.* **15** (2000) R55.

[47] H.-K. Lee, T.-S. Suh, B.-Y. Choe, K.-S. Shinn and G.-S. Cho, *Transient photocurrent in amorphous silicon radiation detectors*, *Nucl. Eng. Technol.* **29** (1997) 468.

[48] B. Fraboni, A. Ciavatti, L. Basiricò and A. Fraleoni-Morgera, *Organic semiconducting single crystals as solid-state sensors for ionizing radiation*, *Faraday Discuss.* **174** (2014) 219.

[49] M. Nakamura and R. Matsubara, *Carrier mobility in organic thin-film transistors: limiting factors and countermeasures*, *J. Photopolym. Sci. Technol.* **27** (2014) 307.

[50] Y.-C. Chang, C.-Y. Wei, Y.-Y. Chang, T.-Y. Yang and Y.-H. Wang, *High-mobility pentacene-based thin-film transistors with synthesized strontium zirconate nickelate gate insulators*, *IEEE Trans. Electron Devices* **60** (2013) 4234.

[51] https://www.sigmaaldrich.com/IN/en/product/aldrich/698423.

[52] O.D. Jurchescu, J. Baas and T.T.M. Palstra, *Effect of impurities on the mobility of single crystal pentacene*, *Appl. Phys. Lett.* **84** (2004) 3061.

[53] C.-Y. Chang, Y.-C. Chang, W.-K. Huang, W.-C. Liao, H. Wang, C. Yeh et al., *Achieving high efficiency and improved stability in large-area ITO-free perovskite solar cells with thiol-functionalized self-assembled monolayers*, *J. Mater. Chem. A* **4** (2016) 7903.

[54] Y.S. Lee, J.H. Park and J.S. Choi, *Electrical characteristics of pentacene-based Schottky diodes*, *Opt. Mater.* **21** (2003) 433.

[55] S. Kasap, J.B. Frey, G. Belev, O. Tousignant, H. Mani, L. Laperriere et al., *Amorphous selenium and its alloys from early xeroradiography to high resolution X-ray image detectors and ultrasensitive imaging tubes*, *Phys. Status Solidi* **246** (2009) 1794.

[56] M.J. Berger, *Photon Cross Sections Database. NIST Standard Reference Database 8 (XGAM)*, http//physics.nist.gov/PhysRefData/Xcom/Text/XCOM.html, 1998.

[57] O.V. Mikhnenko, P.W.M. Blom and T.-Q. Nguyen, *Exciton diffusion in organic semiconductors*, *Energy Environ. Sci.* **8** (2015) 1867.

[58] M. Shah, M.H. Sayyad and K.S. Karimov, *Electrical characterization of the organic semiconductor Ag/CuPc/Au Schottky diode*, *J. Semicond.* **32** (2011) 44001.

[59] A. Ciavatti, *Transport Properties and Novel Sensing Applications of Organic Semiconducting Crystals*, Ph.D.thesis, Alma Mater Studiorum — Università di Bologna (2015) [DOI: 10.6092/UNIBO/AMSDOTTORATO/6769].

[60] U. Zschieschang, F. Ante, T. Yamamoto, K. Takimiya, H. Kuwabara, M. Ikeda et al., *Flexible low-voltage organic transistors and circuits based on a high-mobility organic semiconductor with good air stability*, *Adv. Mater.* **22** (2010) 982.

[61] A.A. Günther, J. Widmer, D. Kasemann and K. Leo, *Hole mobility in thermally evaporated pentacene: Morphological and directional dependence*, *Appl. Phys. Lett.* **106** (2015) 233301.

[62] F. Ravotti, *Dosimetry techniques and radiation test facilities for total ionizing dose testing*, *IEEE Trans. Nucl. Sci.* **65** (2018) 1440.

[63] R.S. Sussmann, *CVD Diamond for Electronic Devices and Sensors*, John Wiley & Sons (2009).

[64] D.R. Kania, M.I. Landstrass, M.A. Plano, L.S. Pan and S. Han, *Diamond radiation detectors*, *Diam. Relat. Mater.* **2** (1993) 1012.

[65] R.D. McKeag, R.D. Marshall, B. Baral, S.S.M. Chan and R.B. Jackman, *Photoconductive properties of thin film diamond*, *Diam. Relat. Mater.* **6** (1997) 374.

[66] R. Zhuang, X. Wang, W. Ma, Y. Wu, X. Chen, L. Tang et al., *Highly sensitive X-ray detector made of layered perovskite-like (NH 4) 3 Bi 2 I 9 single crystal with anisotropic response*, *Nat. Photonics* **13** (2019) 602.

[67] T. Agostinelli et al., *Space charge effects on the active region of a planar organic photodetector*, *J. Appl. Phys.* **101** (2007) 114504.

[68] V.D. Mihailetchi, J. Wildeman and P.W.M. Blom, *Space-charge limited photocurrent*, *Phys. Rev. Lett.* **94** (2005) 126602.

[69] C.A. Mills et al., *Direct detection of 6 MV X-rays from a medical linear accelerator using a semiconducting polymer diode*, *Phys. Med. Biol.* **58** (2013) 4471.

[70] S. Lai, P. Cosseddu, L. Basiricò, A. Ciavatti, B. Fraboni and A. Bonfiglio, *A Highly Sensitive, Direct X-Ray Detector Based on a Low-Voltage Organic Field-Effect Transistor*, *Adv. Electron. Mater.* **3** (2017) 1600409.